

Performance and Loss Analyses of High-Efficiency CBD-ZnS/Cu(In_{1-x}Ga_x)Se₂ Thin-Film Solar Cells

Alexei Pudov¹, James Sites¹, Tokio Nakada²

¹ Department of Physics, Colorado State University, Fort Collins, Co, 80523, USA

² Department of Electrical Engineering and Electronics,
Aoyama Gakuin University, Setagaya-ku, Tokyo 157-8572, Japan

(Received)

KEYWORDS: ZnS buffer, Cu(In,Ga)Se₂, thin-film solar cells, loss analysis, ZnO

ABSTRACT

Chemically deposited ZnS has been investigated as a buffer layer alternative to CdS in polycrystalline thin-film Cu(In_{1-x}Ga_x)Se₂ (CIGS) solar cells. Cells with efficiency of up to 18.1 % based on CBD-ZnS/CIGS heterostructures have been fabricated. This paper presents the performance and loss analyses of these cells based on the current-voltage (J-V) and spectral response curves, as well as comparisons with high efficiency CBD-CdS/CIGS and crystalline silicon counterparts. The CBD-ZnS/CIGS devices have effectively reached the efficiency of the current record CBD-CdS/CIGS cell. The effects of the superior current of the ZnS cell and the superior junction quality of the CdS cell on overall performance nearly cancel each other.

Thin-film solar cells with Cu(In_{1-x}Ga_x)Se₂ (CIGS) absorbers have achieved high efficiencies in recent years. Cadmium sulfide (CdS) buffer layers prepared by chemical bath deposition (CBD) are commonly used in CIGS-based cells. Even though cells with the ZnO/CBD-CdS/CIGS structure have high efficiencies, manufacturing companies have sought alternatives to the CBD-CdS buffer layer, which could eliminate the use of Cd and improve the collection of carriers generated by short-wavelength light. One promising alternative material is ZnS. Its band-gap energy (E_g) of 3.8 eV makes it transparent to practically all wavelengths of the solar spectrum. In contrast CdS, with its band gap of 2.4 eV, is highly absorbing for wavelengths below 520 nm. There has been a considerable progress in using CBD-ZnS in CIGS-based thin-film solar cells^{1,2}. ZnO/CBD-ZnS/CIGS solar cells with efficiency of up to 18.1 % have been fabricated at Aoyama Gakuin University. We present the performance and loss analyses³ of these cells and also two CBD-CdS/CIGS and Si comparison cells made elsewhere.

CBD-ZnS buffer layers were chemically grown on CIGS thin films using a ZnSO₄ (0.1-0.3M)-ammonia (5-8 M, PH=10.5-11.0)-thiourea (0.4-0.8 M) aqueous solution at 80°C. X-ray photoelectron spectroscopy (XPS) analysis revealed that the CBD-ZnS film includes a large amount of oxygen in the form of Zn(OH)₂ and ZnO. Therefore, we refer to this material as CBD-ZnS, since it is not pure ZnS, although its optical band-gap energy is very close to the 3.8-eV single-crystal value.

The detailed fabrication process of a MgF₂/ZnO:Al/CBD-ZnS/CIGS/Mo/soda-lime glass solar cell is described elsewhere^{1,2}. The J-V characteristics were measured at the Japan Quality Association (JQA) using a solar simulator under AM 1.5, 100 mW/cm² illumination at 24°C. The

active area of the small-size solar cells was carefully measured by means of a digital microscope (KEYENCE, VH6300). The solar cell was annealed in air at 200°C for 10 minutes, and measured after light-soaking for 5 min. The best CIGS solar cell with a CBD-ZnS buffer layer yielded an active area efficiency of 18.1% with $V_{oc} = 0.671$ V, $J_{sc} = 34.7$ mA/cm², FF = 0.7764, and an active area of 0.15 cm².

Figure 1 compares the current density vs. voltage (J-V) plotted linearly, the log of forward current, and the quantum efficiency (QE) characteristics of three high-efficiency solar cells. One cell is the highest efficiency thin-film CBD-ZnS/CIGS cell made at Aoyama Gakuin University (AGU), one is the highest efficiency thin-film CBD-CdS/CIGS cell from the U.S. National Renewable Energy Laboratory (NREL) ⁴⁾, and the third is a very high efficiency crystalline Si cell from the University of New South Wales (UNSW) ⁵⁾. As can be seen from Fig. 1a, the two CIGS cells have very similar looking J-V curves and nearly identical current and voltage intercepts. This similarity, however, is misleading, and will be discussed below.

Figure 1b plots the same data as Fig. 1a. The data is shifted by the short circuit current (J_{sc}), corrected for the shunt resistance (r_{sh}), and plotted on an exponential scale. The inverse slope of each of these curves is AkT , where A is the diode quality factor. The two CIGS cells have an A -factor near 1.5, whereas that of the Si cell is near the ideal value of 1.0. The CBD-ZnS/CIGS cell has a slightly higher A value than the CBD-CdS/CIGS cell, which leads to slightly lower maximum power voltage (V_{mp}). The short-wavelength QE response of the ZnS/CIGS cell (Fig. 1c) is clearly superior to the CdS/CIGS cell, which is consistent with the larger band gap of the CBD-ZnS. The QE curves, however, also show a significant difference in their fall-off at long wavelengths, indicating an absorber band gap of 1.12 eV for the CdS/CIGS and the Si cells, but 1.19 eV for the ZnS/CIGS cell. The fact that a larger open-circuit voltage V_{oc} is not realized for the higher band-gap CBD-ZnS cell implies that it is somewhat lower in junction quality. A potential cause of the lower junction quality is that the CBD-ZnS cells did not have an un-doped ZnO layer, which protects the junction from plasma damage during ZnO:Al sputter-deposition and is commonly used in CBD-CdS/CIGS devices. Hence, the similar current-voltage curves for the two CIGS cells shown in Fig. 1a should be interpreted as the compensating effects of the superior short-wavelength QE of the CBD-ZnS/CIGS cell and the superior voltage, relative to the absorber band gap, of the CBD-CdS/CIGS cell.

The photocurrent losses of a solar cell (in mA/cm²) can be quantified as shown in Fig. 2, which depicts the QE of the CBD-ZnS/CIGS cell and the AM1.5 global spectrum on a common wavelength axis. The spectrum is expressed as "photon current", where the photon flux at each wavelength (units of photons/s/cm²/nm) is multiplied by unity charge. The photocurrent itself is the product of QE and photon current integrated over wavelength. Each photocurrent loss can similarly be calculated by integrating the appropriate QE loss region multiplied by the photon current ^{3, 6)}. The loss regions shown in Fig. 2 are the front-surface light reflectance and grid shading, window-layer band-gap absorption, front layer glass or transparent conductive oxide (TCO) free electron absorption, and loss of deeply penetrating photons. These losses are enumerated in Table 1 for the three cells studied. The deep-penetration loss region and the free-electron absorption loss region overlap, and the loss from the overlap region is divided between the two effects. The large difference among the cells is the short-wavelength window-layer absorption. This loss is nearly 4 mA/cm² for the CBD-CdS/CIGS cell, about 1 mA/cm² for the CBD-ZnS/CIGS cell, and close to zero for the Si cell.

Table 2 gives a direct comparison of the performance parameters of the CBD-ZnS/CIGS, CBD-CdS/CIGS, and Si cells. It also lists the factors that contribute to the AGU/NREL efficiency

difference and shows numerically the amount and the direction of each difference. Values not listed are nearly the same for the AGU and NREL cells. The AGU cell gains 1.6 % in efficiency compared to the NREL cell because of the short-wavelength photocurrent difference. However, it loses 1.3 % in efficiency due to lower V_{oc} relative to the band gap, 0.4 % due to shunting, 0.2 % due to the A -factor difference, and 0.3 % due to greater free-electron absorption. The total of these differences accounts for the small overall efficiency difference (~ 0.7 %) between the AGU and the NREL cell.

The reported CBD-ZnS/CIGS devices made at Aoyama Gakuin University have very nearly achieved the efficiency of their best CBD-CdS/CIGS (NREL) counterparts. One of the factors that play a primary role in their high performance is the superior short-wavelength current, which results from the high CBD-ZnS band-gap energy. The effects of the superior current of the ZnS cell and the superior junction quality of the CdS cell on overall performance are similar in magnitude and hence nearly cancel each other.

The work at Colorado State University was supported by the U.S. National Renewable Energy Laboratory.

References:

1. T. Nakada and M. Mizutani: to be published in *Jpn. J. Appl. Phys.* (2002).
2. T. Nakada and M. Mizutani, *Proc. 28th IEEE PV Spec. Conf.*, (Anchorage, 2000) p. 529-533.
3. J.R. Sites: *Proc. 12th Photovoltaic Sci. and Eng. Conf.*: (Jeju, Korea, June, 2001) p. 627-630, and *Solar Energy Mat. Solar Cells* (in press).
4. M. Contreras et al., *Progress in Photovoltaics*, **7** (1999) 311-316.
5. M.A Green, J. Zhao, and A. Wang: *Proc. 2nd World Conf. Photovoltaic Energy Conversion* (July, 1998, Vienna, Switzerland) p.1187-1192.
6. G. Stollwerck, M.S. Thesis, Colorado State University, 1995, unpublished.

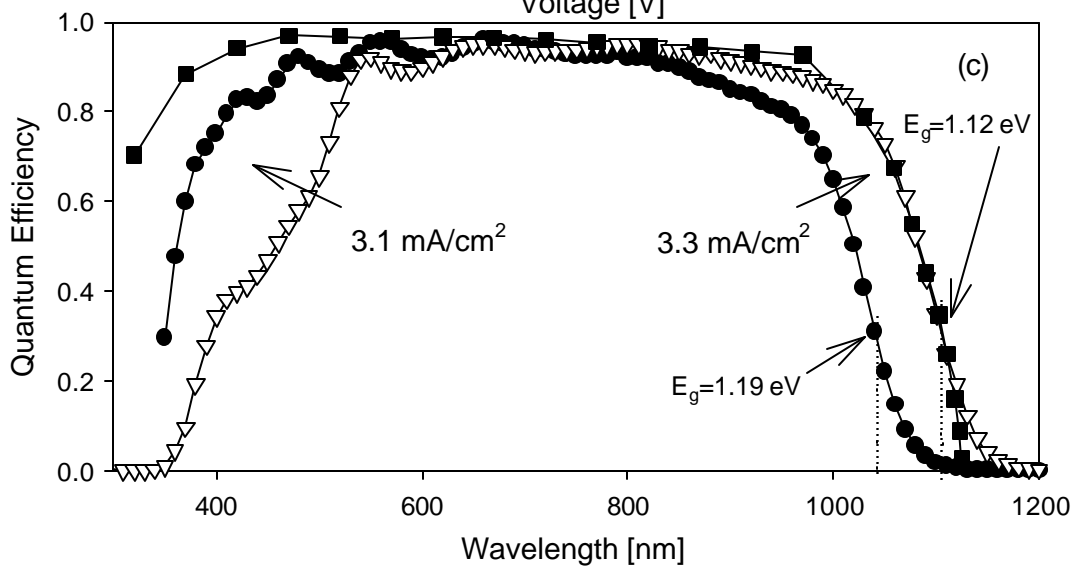
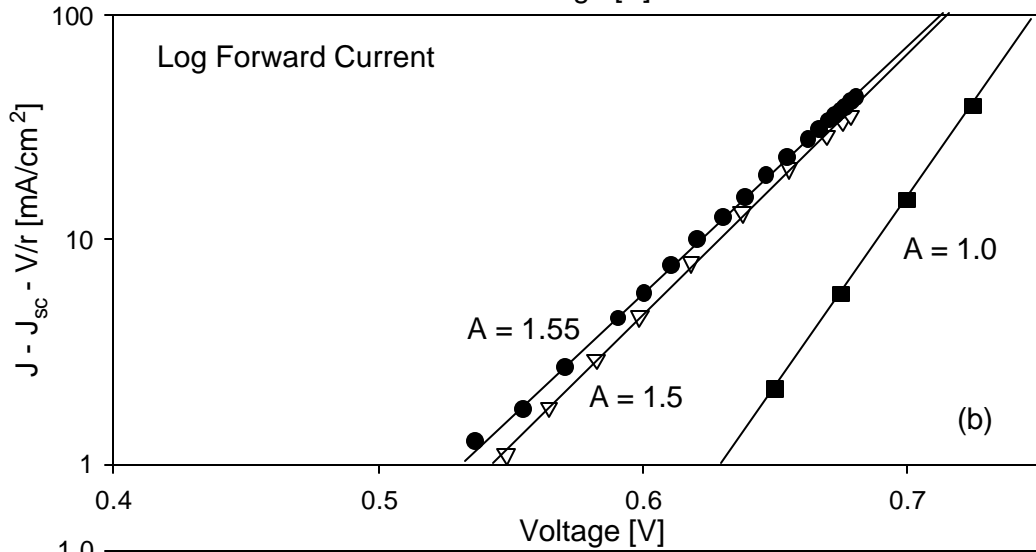
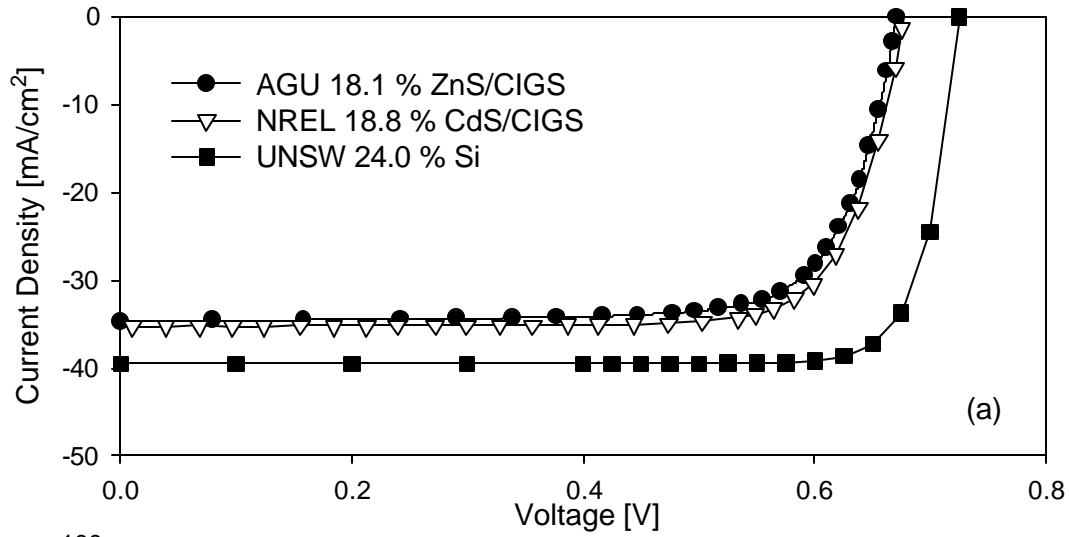
Figure and table captions

Fig. 1. Comparisons in (a) current-voltage, (b) log forward current and (c) quantum efficiency of high efficiency cells. All measurements were carried out at room temperature.

Fig. 2. QE-based photocurrent loss analysis of the AGU cell.

Table 1. Photocurrent comparison (mA/cm^2)

Table 2. Parameter comparison between the three cells.



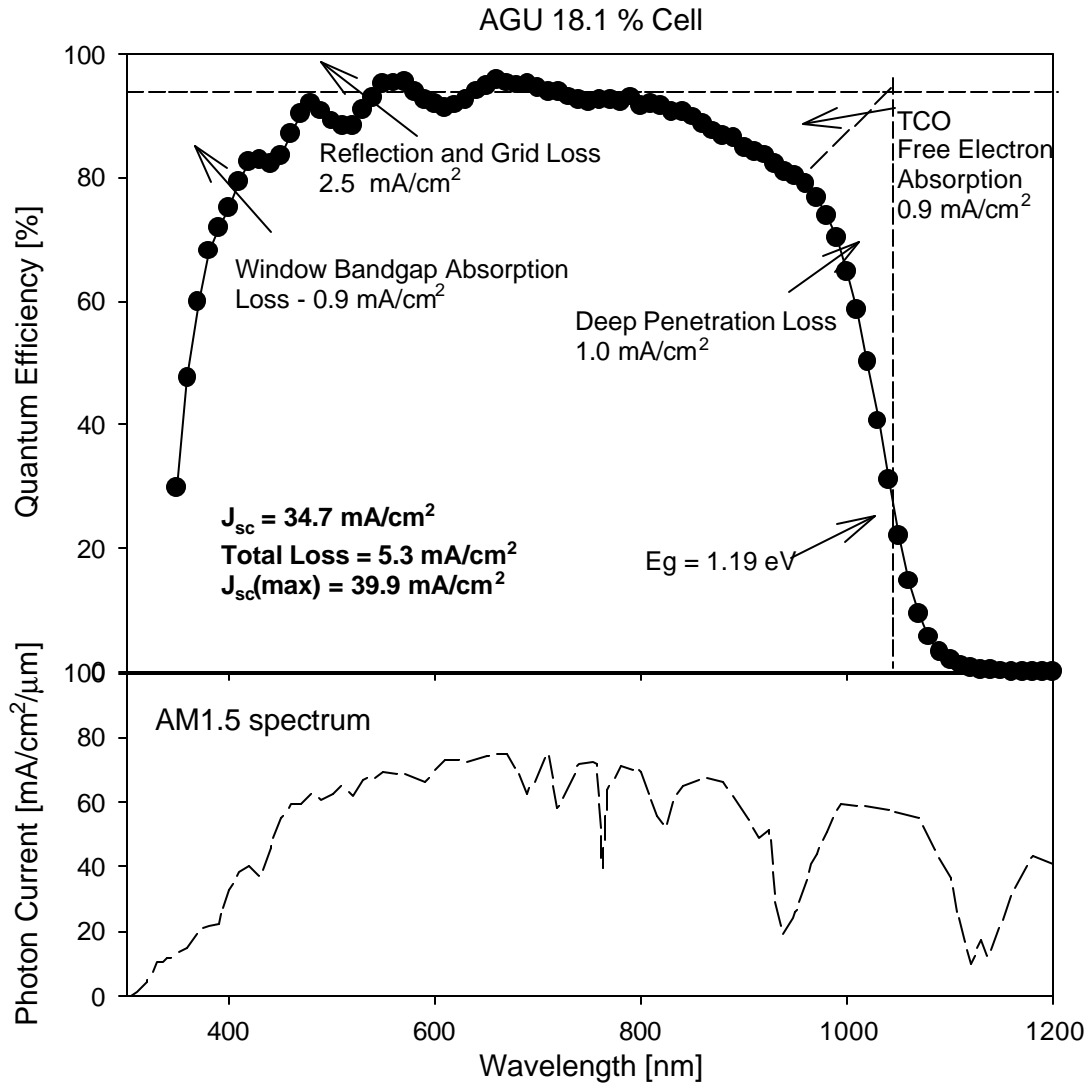


Table 1. Photocurrent comparison (mA/cm²)

| Cell | ZnS/CIGS | CdS/CIGS | Si |
|--|----------|----------|------|
| J_{sc} | 34.7 | 35.2 | 39.5 |
| Front surface losses (reflection and shading) | 2.5 | 2.6 | 1.4 |
| Window absorption loss | 0.9 | 3.9 | 0.2 |
| TCO free electron absorption | 0.9 | 0.6 | 0.6 |
| Deep penetration loss | 1.0 | 1.0 | 1.6 |
| Total loss | 5.3 | 8.1 | 3.8 |
| J_{sc}(max) possible for the band gap | 39.9 | 43.3 | 43.3 |

Table 2. Parameter comparison between the three cells.

| Manufacturer | AGU | NREL | UNSW | h (AGU) – h (NREL) [%] |
|--|------|------|------|---------------------------------------|
| Efficiency [%] | 18.1 | 18.8 | 24.0 | |
| V_{oc} [mV] | 671 | 678 | 725 | |
| J_{sc} [mA/cm²] | 34.7 | 35.2 | 39.5 | |
| FF [%] | 77.6 | 78.6 | 83.8 | |
| J_{sc} from I below 540 nm [mA/cm²] | 7.3 | 4.2 | 7.9 | +1.6 |
| Long wavelength J_{sc} losses [mA/cm²] | 1.9 | 1.6 | 1.6 | -0.3 |
| E_g/q - V_{oc} [mV] | 519 | 442 | 395 | -1.3 |
| r_{sh} [Ω-cm²] | 800 | 3900 | high | -0.4 |
| Diode Quality Factor | 1.55 | 1.5 | 1.0 | -0.2 |